Journal of Solid State Chemistry 219 (2014) 55–66

Contents lists available at ScienceDirect

Journal of Solid State Chemistry

journal homepage: www.elsevier.com/locate/jssc

A set of alkali and alkaline-earth coordination polymers based on the ligand 2-(1*H*-benzotriazol-1-yl) acetic acid: Effects the radius of metal ions on structures and properties

Jin-Hua Wang [a], Gui-Mei Tang [a,*], Ting-Xiao Qin [a], Shi-Chen Yan [a], Yong-Tao Wang [a,*], Yue-Zhi Cui [a], Seik Weng Ng [b]

[a] *Department of Chemical Engineering, Shandong Provincial Key Laboratory of Fine Chemicals, Qilu University of Technology, Jinan 250353, PR China*
[b] *Department of Chemistry, University of Malaya, Kuala Lumpur 50603, Malaysia*

ARTICLE INFO

Article history:
Received 10 March 2014
Received in revised form
27 June 2014
Accepted 5 July 2014
Available online 25 July 2014

Keywords:
Alkali
Alkaline-earth
Photoluminescence
Metal coordination polymers
Ferroelectricity
Second-harmonic generation

ABSTRACT

Four new metal coordination complexes, namely, $[\mathrm{Na}(\mathbf{BTA})]_n$ (**1**), $[\mathrm{K}_2(\mathbf{BTA})_2(\mu_2\text{-}\mathrm{H_2O})]_n$ (**2**), and $[M(\mathbf{BTA})_2(\mathrm{H_2O})_2]_n$ (M=Ca(II) and Sr(II) for **3** and **4**, respectively) [**BTA**=2-(1*H*-benzotriazol-1-yl) acetic anion], have been obtained under hydrothermal condition, by reacting the different alkali and alkaline-earth metal hydroxides with **HBTA**. Complexes **1**–**4** were structurally characterized by X-ray single-crystal diffraction, EA, IR, PXRD, and thermogravimetry analysis (TGA). These complexes display low-dimensional features displaying various two-dimensional (2D) and one-dimensional (1D) coordination motifs. Complex **1** displays a 2D layer with the thickness of 1.5 nm and possesses a topologic structure of a 11 nodal net with Schläfli symbol of $\{3^{18}\}$. Complex **2** also shows a thick 2D sheet and its topologic structure is a 9 nodes with Schläfli symbol of $\{3^{11}\times 4^{2}\}$. Complexes **3** and **4** possess a 1D linear chain and further stack via hydrogen bonding interactions to generate a three-dimensional supramolecular architecture. These results suggest that both the coordination preferences of the metal ions and the versatile nature of this flexible ligand play a critical role in the final structures. The luminescent spectra show strong emission intensities in complexes **1–4**, which display violet photoluminescence. Additionally, ferroelectric, dielectric and nonlinear optic (NLO) second-harmonic generation (SHG) properties of **2** are discussed in detail.

1. Introduction

Over the past decade, considerable attention has been devoted to the rational design and synthesis of metal coordination polymers (MCPs) or metal–organic frameworks (MOFs) owing to their intriguing and charming architectures [1] and their potential applications as functional solid materials in scientific areas such as gas storage/separation [2], catalysis [3], sensing [4], magnetism [5], ferroelectricity [6], optics [7], drug delivery [8], conductivity [9], and clean energy generation [10]. It is well known that the final structures and fascinating properties of the synthesized MCPs can be tuned through altering synthetic variables, for examples, the solvent [11], temperature [12], the molar ratio of metal ions and organic bridging linkers [1c], counter ions [13], the pH value [14], and the metal centers and the organic ligands [15]. Obviously, the metal centers play a crucial role in the final architectures and physical properties [15g,16]. During the construction of MCPs or MOFs, transition metal centers are often chosen because they possess well-known coordination behaviors with carboxylate groups [17]. Compared to these cases, the investigation and development of alkali or alkaline-earth metal coordination polymers (AMCPs) are relatively rare. There exists the following reason: the interaction between alkali or alkaline-earth metal ions with carboxylate oxygen atoms is mainly ionic in nature owing to large differences in electronegativity, which it is uneasy to predict and govern the coordination geometry of the metals. Hence, the systematic studies of AMCPs still remain challenge though some charming structures of AMCPs have been obtained. Despite of difficulties in predicting coordination geometry and carrying out systematic investigations, the incorporation of s-block metal ions/alkali and alkaline-earth metal ions to AMCPs offers several advantages: (i) the relatively high charge density and ionic nature of these metal ions result into strong bonding interaction with carboxylate oxygen atoms; (ii) their low-atomic weight makes AMCPs display gravimetric advantage in the fields of gas storage [18], sensing [19], conductivity [9,20], and battery [21]; (iii) most of them are abundant elements in the earth such as Na, K, Mg, and Ca, which are essential in many biological processes

---

[*] Corresponding authors. Tel.: +86 0531 89631208; fax: +86 0531 89631208.
E-mail addresses: meiguit@163.com (G.-M. Tang), ceswyt@sohu.com (Y.-T. Wang).

http://dx.doi.org/10.1016/j.jssc.2014.07.003
0022-4596/

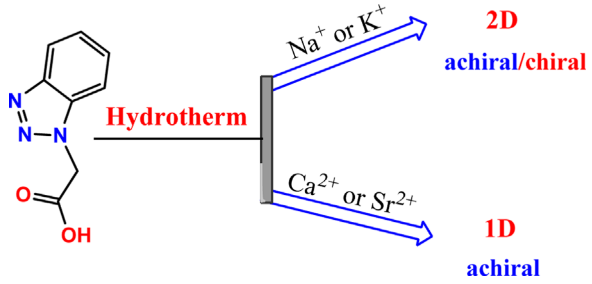

Scheme 1. Self-assemblies of the ligand **HBTA** with a series of alkali and alkaline-earth metal ions.

[22]. Recently, some interesting complexes [23] containing alkali and alkaline-earth ions such as Li [24], Na [25], K [26], Rb [27], Cs [28], Mg [29], Ca [30], Sr [31] and Ba [31d,e,32] have been documented. During the synthetic process of these interesting AMCPs, the choice of functional organic bridging ligands play a key role in construction of AMCPs [33]. It is popular to use some polycarboxylate bridging linkers [23f,34]. However, a few structures and properties based on AMCPs containing *N*-heterocycle carboxylic ligand are still rarely investigated so far [23d,29k,35]. Therefore, the systematic development of AMCPs based on *N*-heterocycle carboxylic ligands still remains challenge.

As a part of our continuous project of the development and investigation of transitional metal coordination polymers (TMCPs) containing azole and *N*-heterocycle carboxylic ligands, which exhibit interesting luminescent, ferroelectric and magnetic properties, we go on designing and constructing TMCPs or AMCPs with fascinating architectures and physic properties. Recently, several TMCPs constructed by a kind of *N*-heterocycle carboxylic linker, 2-(1*H*-benzotriazol-1-yl) acetic acid (**HBTA**, Scheme 1), have been reported by us and other research groups [36]. Two TMCPs containing Zn(II) and Ag(I) are both one-dimensional chain structures [36a,b]; the Zn complex exhibits interesting ferroelectric and luminescent properties [36a]. Motivated by these elegant works, we envision that **HBTA** possesses unsymmetric bridging linker as it contains two functional groups, that is, triazole group and carboxylic one. Thus, it can be explored to provide a convenient access to constructing a set of AMCPs with interesting physical properties under hydrothermal conditions. Herein, we wish to report the syntheses, solid state structures, luminescent, SHG efficiency, dielectric and ferroelectric properties of $[\mathrm{Na}(\mathbf{BTA})]_n$ (**1**), $[\mathrm{K}_2(\mathbf{BTA})_2(\mu_2\text{-}\mathrm{H_2O})]_n$ (**2**), $[M(\mathbf{BTA})_2(\mathrm{H_2O})_2]_n$ (M=Ca and Sr for **3** and **4**, respectively), which were obtained by sodium, potassium, calcium, and strontium hydroxides with unsymmetric bridging ligand **HBTA** under hydrothermal conditions (Scheme 1). Additionally, their TGA were discussed in detail.

2. Experimental section

2.1. Materials and physical measurements

Ligand **HBTA** was prepared according to the literature [36a]. The reagents and solvents employed were commercially available and used as received without further purification. Elemental analyses were performed on an Elementar Vario EL III microanalyser. The FT-IR spectra were recorded from KBr pellets in range 400–4000 $\mathrm{cm^{-1}}$ on a Bruker Tensor 27 spectrometer. The X-ray powder diffraction was recorded on a Bruker D8 Advance diffractometer at 40 kV, 40 mA with a Cu-target tube and a graphite monochromator. 2θ falls in the range of 5–60°. The experimental powder XRD patterns are in good agreement with the corresponding simulated ones (Figs. S1–S4 in the Supporting information) except for the relative intensity variation because of preferred orientations of the crystals. Therefore, the phase purity of the as-synthesized products is substantiated. Solid-state fluorescent studies were conducted at room temperature on an Edinburgh FLS-920 system. Thermogravimetric analysis (TGA) data were collected with a Perkin-Elmer TGS-2 analyzer in N_2 at a heating rate of 10 °C $\mathrm{min^{-1}}$. Kurtz powder SHG measurements were performed on ground samples of crystalline **1–4** with a synchroscan streak camera (Hamamatsu Model C1587, 8 ps resolution) connected to a polychromator as the detector system, and an optical parametric generator (Spectra Physics, Model: OPA-800C) pumped by a mode-locked Ti: sapphire laser oscillator–amplifier system (Spectra Physics, Model: Hurricane) as the pump source. The powder second-harmonic signals were compared to that of KH_2PO_4 to determine the relative SHG efficiencies of **1–4**. The measurement of the polarization-voltage curves were carried out on the powder sample in a pellet form using an aixACCT TF Analyzer 2000 system at room temperature, while the sample has been pressed well into a pellet (diameter of 5 mm and thickness of 1.5 mm) sandwich by silver electrodes and immerged in insulating oil. The measurement of the solubility of compounds **1**–**4** were carried out the powder sample in some solvents. The powder samples were dissolved in the solvents (5 ml) until they were saturated in solution. The solution was shaken for 10 h at 298 K. Then the solution was filtered and the solvents were removed under vacuum. The residue was weighted and its solubility was calculated.

2.1.1. Synthesis of $[\mathrm{Na(BTA)}]_n$ (**1**)

The reaction mixture of **HBTA** (177 mg, 1.0 mmol), NaOH (40 mg, 1 mmol) and water (10 ml) in a 15 ml Teflon reactor, under autogenous pressure at 160 °C for one week and then cooled to room temperature at a rate of 5 °C $\mathrm{h^{-1}}$. Colorless plate crystals of complex **1** suitable for X-ray diffraction analysis were obtained (0.152 g, yield: 70% based on NaOH). Elemental analysis calcd (%) for $C_8H_6N_3NaO_2$ (199.15): C, 48.25; H, 3.04; N, 21.10; found: C, 48.05; H, 3.05; N, 21.02. IR (KBr, $\mathrm{cm^{-1}}$): 3369(w), 3228(w), 3062(m), 3001(m), 2954(w), 2358 (w), 1942(w), 1905(w), 1782(w), 1618(vs), 1496(w), 1456(m), 1431(s), 1404(s), 1323(m), 1290(w), 1263(m), 1226(s), 1168(m), 1136(m), 1116 (w), 1103(m), 999(m), 927(m), 974(m), 916(m), 869(w), 800(m), 781 (m), 769(m), 742(s), 702(m), 665(m), 621(m), 586(m), 572(w), 430(m).

2.1.2. Synthesis of $[\mathrm{K_2(BTA)_2}(\mu_2\text{-}\mathrm{H_2O})]_n$ (**2**)

The preparation of **2** was similar to that of **1** except that KOH (55 mg, 0.50 mmol) was used instead of NaOH. Colorless needle crystals of **2** were collected in a 73% yield (based on KOH). Elemental analysis calcd (%) for $C_{16}H_{14}K_2N_6O_5$ (448.53): C, 42.85; H, 3.15; N, 18.74; found: C, 42.99; H, 3.13; N, 18.68. IR (KBr, $\mathrm{cm^{-1}}$): 3421(br), 3398 (br), 3061(w), 3001(w), 2904(w), 1940(w), 1867(w), 1826(w), 1772(w), 1618(vs), 1560(w), 1541(w), 1502(w), 1456(w), 1429(m), 1400(s), 1321 (s), 1263(w), 1224(s), 1168(m), 1101(m), 995(w), 974(w), 929(w), 802 (m), 773(w), 744(s), 700(m), 663(m), 621(w), 588(w), 538(w), 476(w), 426(w).

2.1.3. Synthesis of $[\mathrm{Ca(BTA)_2(H_2O)_2}]_n$ (**3**)

The reaction mixture of $CaCl_2$ (56 mg, 0.5 mmol), HBTA (177 mg, 1.0 mmol), NaOH (40 mg, 1 mmol) and water (10 ml) in a 15 ml Teflon reactor, under autogenous pressure at 160 °C for one week and then cooled to room temperature at a rate of 5 °C $\mathrm{h^{-1}}$. Pale-yellow needle crystals of complex **3** suitable for X-ray diffraction analysis were obtained (0.152 g, yield: 70% based on $CaCl_2$). Elemental analysis calcd (%) for $C_{16}H_{16}CaN_6O_6$ (428.43): C, 44.86; H, 3.76; N, 19.62; found: C, 44.71; H, 3.74; N, 19.71. IR (KBr, $\mathrm{cm^{-1}}$): 3495(vs), 3317(w), 3280(w), 3201(m), 3034(w), 2997(m), 2962(m), 2835(w), 2750(w), 2270(w), 1654(m), 1587(vs), 1496(m), 1456(m), 1438(s), 1396(s), 1381(w), 1317 (s), 1274(s), 1232(s), 1165(m), 1136(m), 1118(m), 999(m), 975(m), 933 (w), 921(m), 842(w), 810(m), 779(m), 765(m), 744(s), 705(m), 665(m), 626(m), 597(m), 536(m), 511(), 430(m).